REPORT DOCUMENTATION PAGE

Form Approved
OMB No. 0704-0188

1. REPORT DATE *(DD-MM-YYYY)*	**2. REPORT TYPE**	**3. DATES COVERED** *(From - To)*
14-11-2011	Final Report	15-08-2010 - 14-08-2011

4. TITLE AND SUBTITLE

Relating Chemical and Topographical Modification of Materials to Macroscopic Adhesion

5a. CONTRACT NUMBER
NA

5b. GRANT NUMBER
FA9550-10-1-0386

5c. PROGRAM ELEMENT NUMBER

6. AUTHOR(S)

Frank Palmieri, Christopher Wohl, Marcus Belcher, John Connel

5d. PROJECT NUMBER

5e. TASK NUMBER

5f. WORK UNIT NUMBER

7. PERFORMING ORGANIZATION NAME(S) AND ADDRESS(ES)

National Institute of Aerospace, 100 Exploration Way, Hampton, VA 23666

8. PERFORMING ORGANIZATION REPORT NUMBER

NA

9. SPONSORING / MONITORING AGENCY NAME(S) AND ADDRESS(ES)

Air Force Office of Scientific Research
875 North Randolph St.
Arlington, VA 22203

10. SPONSOR/MONITOR'S ACRONYM(S)

11. SPONSOR/MONITOR'S REPORT NUMBER(S)
AFRL-OSR-VA-TR-2012-0795

12. DISTRIBUTION / AVAILABILITY STATEMENT

Distribution A - Approved for public release

13. SUPPLEMENTARY NOTES

14. ABSTRACT

Adhesive bonding offers many advantages over mechanical fastening, but requires major improvements in reliability and predictability before it can be incorporated in primary structures for aviation transport. Surface treatment is widely recognized as the single most important process for attaining robust, predictable bonds. This report documents the preliminary testing of a laser ablation technique for the pre-treatment of titanium and carbon fiber reinforced composite adherends. Laser ablation imparts both topographical and chemical changes to the adherend surface which can lead to strong and durable bonds. The relationship between topographical and chemical modifications created by laser treatment and the resulting adhesive properties of mechanical test specimens are investigated. Surface roughness and chemical species were analyzed using microscopy, goniometry, and spectroscopic techniques. Mechanical tests included single lap shear specimens of both titanium and composite adherends. Some promising results show improvements in strength and durability for laser treated lap shear specimens compared to baseline values.

15. SUBJECT TERMS

16. SECURITY CLASSIFICATION OF:			**17. LIMITATION OF ABSTRACT**	**18. NUMBER OF PAGES**	**19a. NAME OF RESPONSIBLE PERSON**
a. REPORT	**b. ABSTRACT**	**c. THIS PAGE**			Dr. Frank L. Palmieri
U	U	U	UU	20	**19b. TELEPHONE NUMBER** *(include area code)* (757) 864 8802

Relating Chemical and Topographical Modification of Materials to Macroscopic Adhesion: Final Report

Authors

Frank L. Palmieri, Chris J. Wohl, Marcus A. Belcher, John W. Hopkins, Guillermo Morales, John W. Connell

1.0 Abstract:

Adhesive bonding offers many advantages over mechanical fastening, but requires major improvements in reliability and predictability before it can be incorporated in primary structures for aviation transport. Surface treatment is widely recognized as the single most important process for attaining robust, predictable bonds. This report documents the preliminary testing of a laser ablation technique for the pre-treatment of titanium and carbon fiber reinforced composite adherends. Laser ablation imparts both topographical and chemical changes to the adherend surface which can lead to strong and durable bonds. Laser surface preparation provides an alternative to the state-of-the-art chemical-dip, peel-ply and grit blast treatments which are expensive, hazardous, and less repeatable than an automated laser ablation technique. The focus of this study is the relationship between topographical and chemical modifications created by laser treatment and the resulting adhesive properties of mechanical test specimens. Surface roughness and chemical species were analyzed using specialized microscopy, goniometry, and spectroscopic techniques. Mechanical tests included single lap shear specimens of both titanium and composite adherends. Some promising results show improvements in strength and durability for laser treated lap shear specimens compared to baseline values. Chemical analysis showed definite trends for the removal of and appearance of specific chemical species as laser ablation power and pattern density was varied. Alternative mechanical tests are being considered to generate the quantitative results required in a general model relating macroscopic adhesion and adherend surface preparation technique.

2.0 Introduction:

Adhesive bonds are critical to the integrity of built-up structures. Currently, disbonds can often be detected, but the strength of adhesion between surfaces in contact is not obtainable without destructive testing. Advancement in the understanding of distinct relationships between surface chemical composition, topography, and interfacial interactions would enable researchers to rapidly generate materials with predetermined or predictable materials properties, such as adhesive bond strength.

2.1 State-of-the-Art Surface Treatment Techniques / Background

State-of-the-art surface treatment techniques for adhesive bonding typically involve modification of surface chemistries and topographies in a low-fidelity fashion. For example, grit-blasting is often used to roughen adherend surfaces prior to bonding. Alternative techniques resulting in changes to topography include manual abrasion and templating methods (such as peel-ply treatments),[1] among others. It is also understood that surface energy of an adherend plays a role in bond performance. Methods to impart changes predominantly in the surface chemistry of the adherends mostly involve chemical or plasma surface treatment.[2] For titanium surfaces, these treatments are necessary to remove a surface passivating titanium oxide layer and typically involve Pasa-Jell® or sol-gel processes that are time consuming, highly variable, and use hazardous chemicals.[3] Furthermore, these treatments introduce an additional interface between the pristine substrate and the chemically modified substrate which can then be a source of bond compromise.[4] These techniques involving surface chemical and topographical modifications of adhesive specimens have been evaluated by our lab.[5-8] Conclusions drawn from these works all indicate that alternative surface treatment methodologies may yield more reliable surfaces for adhesive bonding.

2.2 Laser Ablative Technique

An alternative method for surface treatment involves the use of laser irradiation. In most reported applications, the laser is utilized to “clean” the surface of residual organics or other debris prior to bonding (i.e., the surface topography is not altered by laser irradiation).[9] Although not intentional, in some instances the surface energy has been altered as indicated by changes in the contact angle a solvent makes with the treated surface.[10] This technique has been demonstrated to be an effective method for adherend surface treatment chemically, but it does not enhance adhesive interactions topographically and further, is not intended to alter the surface chemistry. Therefore, any fortuitous adhesion-promoting changes to the substrate surface chemistry were not expected and thus, not examined. Previous research using laser irradiation to alter surface topography for adhesion promotion has been conducted using nonspecific ablation processes relying on differences in ablation thresholds and rates to generate topographies.[11-14]

2.3 Adherend Initial Conditions

In this study, the native roughness of the adherend surface was considered for both CFRP and titanium. CFRP manufactured by molding in contact with breather and release fabrics created dimpled surfaces with large topographies relative to the features created by grit blasting or

laser ablation. The surface dimpling was removed from the panels by replacing the fabric components of the lay-up with smooth Kapton® film laid directly against the polished surface of the mold. Panels molded against Kapton® film had native roughness at least an order of magnitude less than the values important to these experiments. The native titanium surface was delivered with about 1 µm of root-mean-square (RMS) roughness. This was removed before any experimental surface treatments were begun by polishing the surface to about 0.05 to 0.08 µm RMS roughness. The polished surfaces were also fully characterized for baseline properties.

2.5 Surface Chemical Properties

Effective adherend surface treatment methods result from increased surface energies presumably matching the surface energy of the adhesive. A material's surface energy depends on both surface chemical composition and topography. The chemical composition changes the surface energy due to intermolecular forces (van der Waals and Lewis acid/base interactions) between surface chemical constituents at an interface.[15] More polar chemical moieties at an interface can precipitate stronger, higher-energy interactions with neighboring molecules than non-polar groups. Surface roughness has long been understood to increase the surface energy of a material.[16] Topographical variation changes the surface energy in two ways. First, increased topographical features (i.e., increased roughness) result in increased surface area, thus providing a greater interaction area relative to a flat substrate. Second, the topographical features themselves can physically induce wetting by creating capillaries. Topographical modifications can also change the surface chemistry of a material. For example, grit blasting erodes surface material. This erosion process results from the breaking of chemical bonds leaving behind reactive surface functionalities. Changes in topography can also promote adhesive interactions due to mechanical interlocking at the interface.

2.6 Project Description

In this report, carbon-fiber reinforced plastic (CFRP, T800H/3900-2) and titanium alloy (Ti-6Al-4V) surfaces are presented, before and after surface treatment, using a number of surface characterization techniques and experiments designed to measure adhesive interactions. The efficacy of these strategies to identify relationships between macroscopic adhesive interactions and surface chemistry and topography was considered, and experimental strategy was modified as needed. The report addresses two fundamental questions: 1) How does laser ablation change surface chemistry and topography to promote favorable adhesive interactions? 2) Can a laser surface treatment be developed to improve adhesive to adherend bonding?

Macroscopic adhesion testing relied upon lap-shear mechanical testing to correlate the apparent shear strength and failure modes with adherend surface pretreatment. To some degree, the productivity and scope of experiments were limited by issues obtaining the full funding needed to fabricate mechanical test specimens. The fabrication of composite lap-shear specimens was modified from the standard process by eliminating gross surface topographical variation from the starting adherend. The modified layup and resulting CFRP adherend roughness reduction is described in this report. For titanium lap-shear specimens, the fabrication process was modified by adding a lapping process to adherend surface preparation

before laser ablation. Lapping of titanium has several beneficial aspects for this experiment including: removal of the native titanium oxide surface layer, reduction of native surface roughness and removal of organic surface contamination.

Microscopic changes in surface chemistry were analyzed using X-ray photoelectron spectroscopy (XPS). In addition, contact angle goniometry was used to measure the changes in surface energy caused by laser ablation.

During the course of the study, it became apparent that peel mode mechanical tests such as the cantilever beam and wedge-crack tests may be useful to study the critical interfacial adhesion region directly. A fracture mechanics analysis indicated that crack extension may be localized to an interface by carefully selecting a mechanical test configuration and adhesive type. As the crack is localized to the interface, a quantitative relationship between surface treatment and fracture energy may be obtained.

3.0 Experimental:

Titanium alloy (Ti-6Al-4V, an alloy consisting of 90% titanium, 6% aluminum and 4% vanadium, 0.063" thick) was purchased from California Metal & Supply, Inc. For lap shear mechanical testing, a modified configuration as called for in ASTM D1002-05 allowed for the use of existing bonding apparatus. Each set of two coupons was treated with an experimental surface preparation technique and bonded immediately. After bonding, some samples were aged in boiling water for 3 days while others were stored in a dessicator until testing.

3.1 Adherend baseline preparations

Titanium adherend coupons were polished using a semi-automated lapping machine (Buehler Automet 3) with a 12” rotating platen. Silicon carbide lapping discs from 240 to 1200 grit were used to flatten and coarsely polish the substrates. The adherends were polished in a series of three minute lapping cycles with the platen rotation direction being alternated after every cycle and no less than four cycles completed at each grit stage. The adherends were visually inspected at various intervals to gauge the completion of each grit stage based on polish uniformity and surface finish. Additional polishing cycles were performed until a consistent surface finish was achieved. A fine polishing slurry of 0.05 µm colloidal alumina achieved the final polish requirement of 0.05 to 0.08 µm RMS roughness. Completion of the slurry stage was decided when the adherend appeared to have a mirror finish with minimal visible scratches.

CFRP panels were prepared in a 12” by 12” format with 16 plys of unidirectional T800H/3900-2 prepreg sheets obtained from Toray of America Inc. Curing was carried out in a vacuum press oven at 350 °F and 100 psi. The prepreg sheets were laid-up in direct contact with Kapton® film in place of breather and release fabrics normally used. Mold release agents were not required for the removal of the Kapton® film from the cured CFRP which was peeled from the cured panel surface manually. Panels were inspected using by ultrasound to ensure proper consolidation before machining into 2, 100 x 200 mm (4” by 8”) pieces.

3.2 Laser Ablation

Laser ablation was performed using a frequency-tripled, neodymium/yttrium aluminum garnet (Nd/YAG) pulsed laser source (λ =355 nm) with a nominal peak output of 7 W. A Photomachining Inc. system provided the necessary beam focusing, steering, and adjustment capability to obtain an approximately 25 µm, circular spot size. The pulse frequency and scan speed were set to 80 kHz and 254 mm/s, respectively for all experiments. The ablation pattern, pitch (line spacing), and power were altered as experimental variables. Experimental powers ranged from 20 mW to 1700 mW as measured by an external power sensor 3A-SH low power thermopile and Nova II Display power meter both from Ophir Spirocon. Pitch was varied from 12.7 to 50 µm. Both titanium and CFRP specimens were ablated only in the area needed for bonding as shown in Figure 1. Ablation patterns were parallel lines on all mechanical test samples. Crosshatch and sparser line arrays were prepared for other non-destructive tests due to a limited number of test specimens that could be produced.

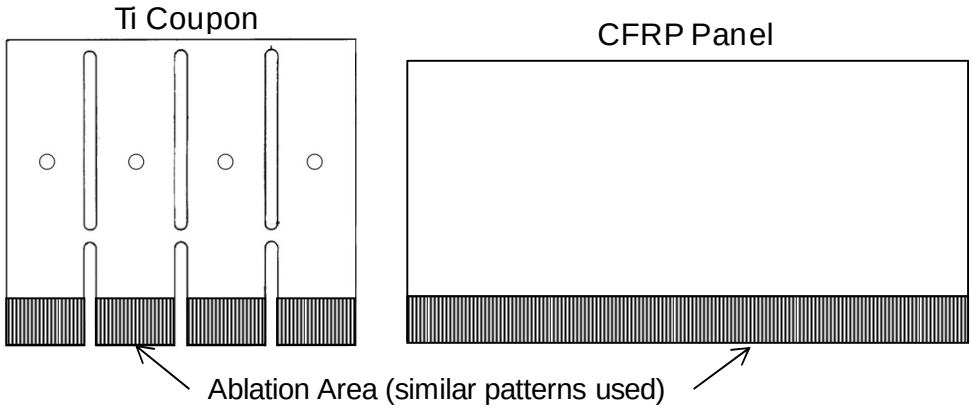

Figure 1: Ablation site and pattern sketch on titanium and composite samples.

3.3 Bonding

Bonding was carried out in a heated press at atmospheric pressure, and cooling was accelerated by blowing compressed air between the press platens. CFRP samples bonded with 3M® AF555 structural adhesive were loaded to about 50 psi and heated to 350 F for two hours. Bond lines were shimmed using stainless steel sheets to control the bond line thickness between 300 and 400 µm. Titanium samples were bonded using PETI-5 adhesive prepared in house using a modification of previously reported work.[20] The samples were loaded to between 45 and 60 psi and heated to 700 °F for one hour. Bond line thickness was controlled between 200 and 300 µm using stainless steel and titanium shims and was measured with a micrometer.

3.4 X-ray Computed Tomography

Bonded composite specimens were examined by x-ray computed tomography (CT) through the lap joint to measure properties of the bond such as void content and bond thickness. CT image analysis was performed using custom software to build a 3D image of the bondline. Image J software was then used to threshold each 3D image as a series of 2D slices and determine the

relative void and bond volumes by counting individual voxels. Instrument resolution allowed for a minimum voxel size of 17 µm.

3.5 Mechanical Testing and Analysis

Tensile testing of titanium SLS specimens was carried out on an Instron 10K test stand fitted with a 5000 lb load cell in accordance with ASTM D 1002 guidelines. Samples were fixed using a pin chuck and spring clip. The strain rate was 0.05 in/min for all tests.

CFRP lap shear specimens were tested using a MTS axial torsional 5 kip test stand following the guidelines provided in ASTM D 3165. Specimen mounting was accomplished using hydraulic grips with CFRP shims. Samples were tested at room temperature.

Failure mode analysis for titanium specimens was performed by collecting images of the failed specimen surfaces with Kodak Easy Share C813 digital camera. Reflective (exposed, polished titanium) surfaces were separated from dark (adhesive covered) areas using a hue, saturation and brightness threshold algorithm in Image J software. Image J was then used to count the number of pixels included in the light areas and the total number of pixels in the failed lap joint. Both adherends for each specimen were characterized in this manner to obtain the percentage of the bond that underwent adhesive failure (referred to herein as 'percent adhesive failure').

3.6 Microscopy

A Zeiss LSM5 Exciter scanning confocal microscope was used to image and measure topography on composite panels. A Zygo Newview 6000 microscope interferometer was used to image and measure topography on the titanium coupons. An Amray 1700 Turbo scanning electron microscope was used as an alternative inspection when imaging using the confocal microscope became difficult due to steep angled features and highly rough surfaces. Samples for SEM inspection were coated with 5 nm of Pd/Au to dissipate charge.

3.7 Goniometry

Contact angles and surface energies were measured using a contact angle goniometer from First Ten Angstroms. Water, ethylene glycol and methylene iodide were three fluids used to measure surface energy on all adherend surfaces. For working with uncured adhesives, methylene iodide was replaced with glycerol to prevent absorption of the probe fluid into the test sample. Some tests resulted in very low contact angles that could not be measured. In these cases, a contact angle of less than 5 degrees was recorded.

3.8 X-ray Photoelectron Spectroscopy

X-ray photoelectron spectroscopy (XPS) spectra were recorded in the Nanomaterials Characterization Center (NCC) at Virginia Commonwealth University on a Thermo Scientific ESCALAB 250 spectrometer with a focused monochromatic Al Kα X-ray (1486.6 eV) source. A hemispherical analyzer with a 6-channeltron multichannel detector was used. The incident X-ray beam was 45° off normal to the sample, while the X-ray photoelectron detector was normal to the sample to produce high signal-to-nose ratio. The samples were fixed onto a sample holder with double sticky tape. Since the samples are nonconductive, charge compensation was employed during data collection by using an internal flood gun (2 eV electrons) and a low energy Ar^+ external flood gun. To produce sufficient charge compensation, argon gas pressure

was kept at 1·10-8 mbar during the experiment. Observed binding energies are correlated to the C1s peak at 285 eV. A Large area XL magnetic lens with a 500 um x-ray spot size in constant analyzer energy (CAE) mode was utilized. Pass energy for the CAE was 20 eV for high-resolution spectra, and 150 eV for the survey scans.

4.0 Results and Discussion

The results for CFRP and titanium analysis are separated into two sub-sections. Images of the ablation topography and roughness data is included along with mechanical test data and surface energy measurements. XPS results for both CFRP and titanium are discussed together in sub-section 4.3.

4.1 CFRP Surface Engineering and Mechanical Testing Results

Confocal images in Figure 2A and B show the native surfaces of CFRP specimens before any surface treatments were rendered. Figure 2A is shows the curved surface topography that is generated in the CFRP surface resin by molding against breather and release fabrics. Removal of fabric layers from CFRP panel lay-up allowed the preparation of relatively smooth CFRP panels as seen in Figure 2B. Starting from a smooth surface, laser processing was applied to remove resin from the CFRP surface. Figure 2C shows the edge of an ablated area on a panel that received a dense array of parallel lines running perpendicular to the carbon fiber direction. In this image, the laser path is parallel to the x-axis and the fiber direction is parallel to the y-axis. The image in Figure 2D shows a high magnification image of a low-density line array with clearly defined line widths and depths. The pitch (line-to-line spacing) in Figure 2C was 12.7 µm while the pitch in Figure 2D was 24.5 µm. The minimum dimensions generated by laser processing (between ablated trenches) are seen in Figure 2D at approximately 10 µm.

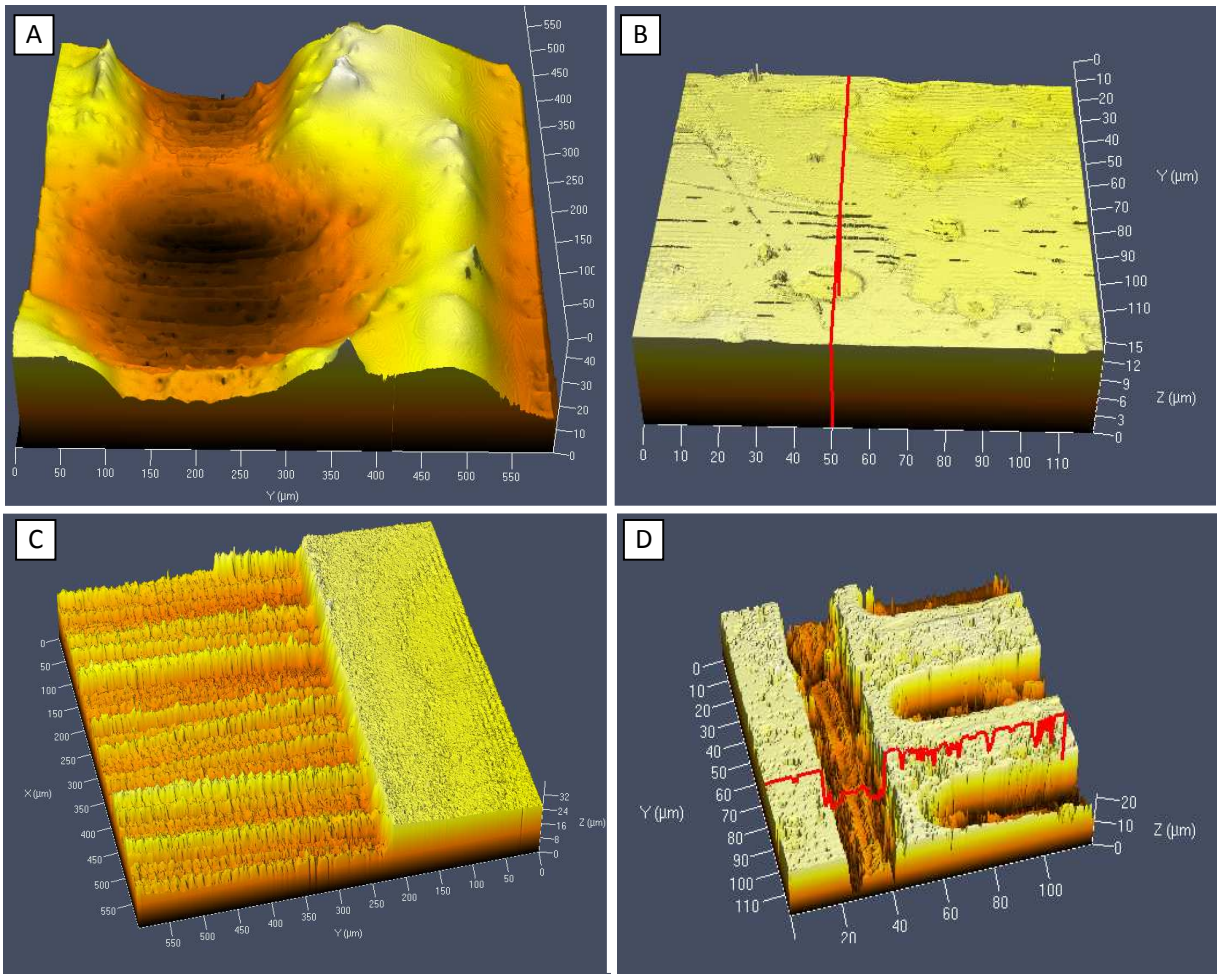

Figure 2: A) Native CFRP surface molded with breather and release fabrics, B) native CFRP surface of a panel molded against Kapton ® directly on the tool surface, C) laser-ablated, dense, parallel lines on CFRP, D) a CFRP panel patterned with parallel lines approaching a border. The ultimate resolution of the system is better than ~10 µm.

The SEM images shown in Figure 3 provide a more accurate description of the laser pattern fidelity. Ablation at 500 mW does not cause any detectable fiber damage although fibers within a few microns of the adherend surface are clearly exposed. Higher magnification shows that the ablated trenches are v-shaped grooves with some minor depth variation probably due to the pulsed laser or proximity of fibers underneath the trench.

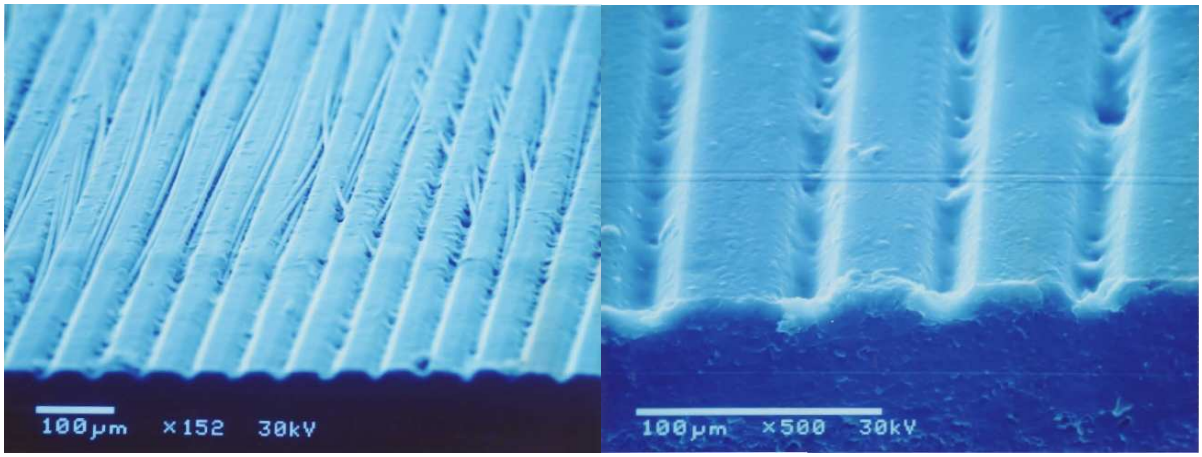

Figure 3: Tilt SEM images of CFRP adherends after ablation at 500 mW with a pitch of 50.8 µm. Left, low magnification with focal plane near image center. Right, high magnification, focused on cross-section area. Edge defects were created during specimen machining.

The CT images of the sample shown in Figure 4 are from ½" overlap, single-lap-shear specimens. The adherends were ablated at 400 mW with a pitch of 12.7 µm on a parallel line pattern with line direction the same as the test loading direction. The excessive void content in the bond lines of the CFRP lap-shear specimens results in little or no valid data from the mechanical testing experiments. The high void content dictates the failure mode of the sample to be cohesive within the adhesive and reduces the apparent shear strength dramatically.

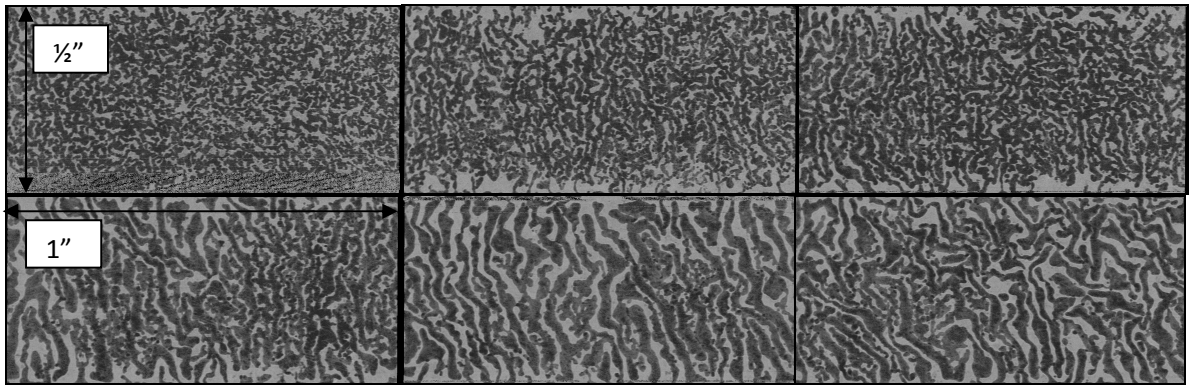

Figure 4: X-Ray computed tomography images taken of a set of 6, 1" wide, CFRP single-lap-shear specimens with ½" overlaps. Each of the six images is a 2x magnification of the ½" by 1" bonded area in the lap joint. Dark areas indicate voids and lighter areas are fully dense adhesive.

The source of the high void content is being explored. Some improvements were noted after bonding sample in an autoclave rather than a heated press. Other adhesives which show no or very low void generation can be employed until the source of the porosity in AF555 adhesive is being determined.

The surface properties and mechanical test results for a set of CFRP samples is shown in Table 1. The native roughness of the CFRP surface was reduced by over an order of magnitude by replacing the breather and release cloths with Kapton® film. Near the ablation threshold, the laser does not induce a significant change in roughness relative to the tool surface. Ablation at 500 mW increases roughness by about one order of magnitude.

Table 1: CFRP Surface Properties and Lap-Shear-Test Results

Sample Name and Adherend Surface Condition	**RMS roughness (nm)**	**Water Contact Angle (deg)**	**Surface Energy (dynes/cm)**	**Average bond line porosity (%)**	**Apparent Shear Strength (psi)**
A. Release/breather fabric	8420	63.6	23.9	Not Tested	Not Tested
B. Tool surface/Kapton®	332	74.2	26.9	Not Tested	4112 ± 205
C. Tool surf., Ablated: 12.7 µm, 25 mW	395	53.1	39.4	13.5	3111 ± 190
D. Tool surf., Ablated: 12.7 µm, 500 mW*	4635	17.2	53.0	36.9	2102 ± 163

*Lap shear specimens were ablated at 400 mW to minimize carbon fiber exposure.

The failed specimens shown in Figure 5 are a side-by-side comparison of the representative failure modes seen for the three sets of tested specimens described in Table 1. The failure mode for all three specimens is dominated by cohesive and thin-layer cohesive failure in the adhesive. The porosity is much higher in both C and D specimens while the pore size is much larger in the D specimen compared to C. Small pores like those in specimen C may be caused by increasing the temperature too quickly during the cure cycle or applying non-constant pressure. More testing is needed to determine the cause of the porosity and how best to eliminate it.

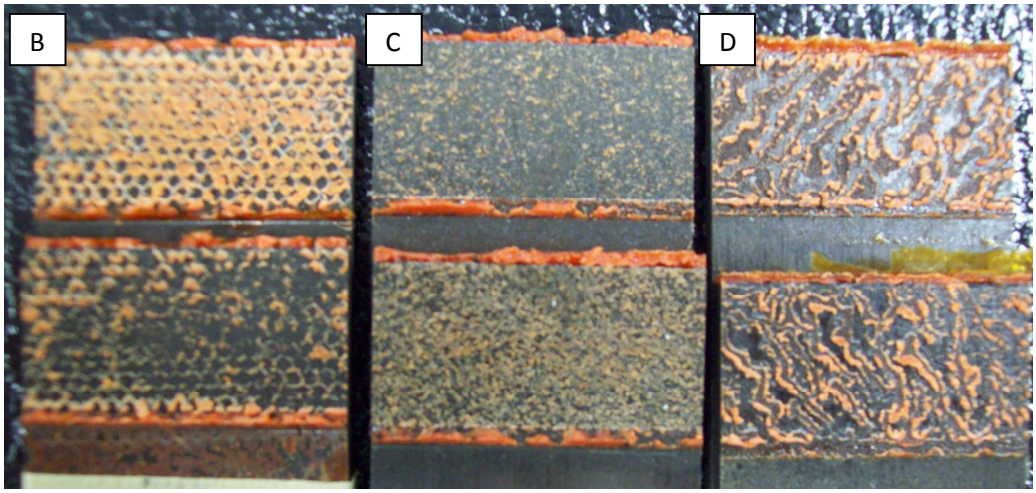

Figure 5: Comparison of CFRP lap-shear failure modes. The B, C, and D labels correlate with the sample names in Table 1.

4.2 Titanium Surface Engineering and Mechanical Testing Results

Titanium ablation samples inspected by a microscope interferometer are shown in Figure 6. Dense lines, isolated lines and crosshatch patterns were prepared at various laser settings to measure the ablation depth, width and material re-deposition. The effects of pattern variation and surface coverage on bond performance was of interest, but the limited number of mechanical test specimens that could be fabricated restricted this work to dense parallel lines like those shown in Figure 6C. The oblique plot in Figure 6D shows the step height obtained when ablating the titanium surface with dense parallel lines. The average ablation depth in this was about 0.5 µm with an average laser power of 1 W.

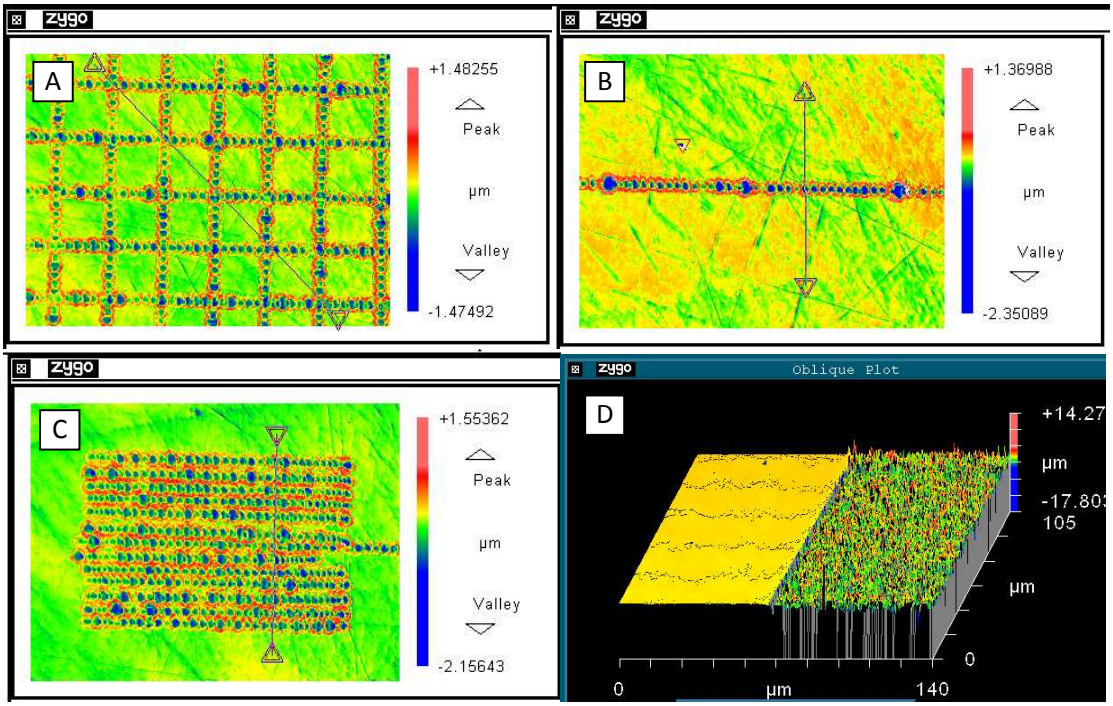

Figure 6: Zygo interferometer images showing the topography generated on titanium coupons by ablating A) a sparse crosshatch pattern, B) an isolated line, C) a dense parallel line pattern (blanket), and D) oblique view of dense parallel lines and the associated step height change at the edge of the ablation area.

Titanium single lap-shear specimens were tested to compare polished surfaces with polished and ablated surfaces. The apparent shear strength, bondline thicknesses and percentage of adhesive failure are shown in Figure 7. The baseline values are measured for samples that received only polishing to a roughness of 50±20 nm RMS. Immersion in boiling water for between 6 and 240 hours resulted in up to 33% loss in apparent shear strength from the baseline samples. Exposure at power (75 mW) at the ablation threshold produced samples with an average apparent shear strength of 4327 psi and about 43% adhesive failure (not shown in Figure 7). At the ablation threshold, samples were expected to undergo laser induced chemical modification with little or no topographical change. The threshold ablation energy did not give desirable apparent shear strengths.

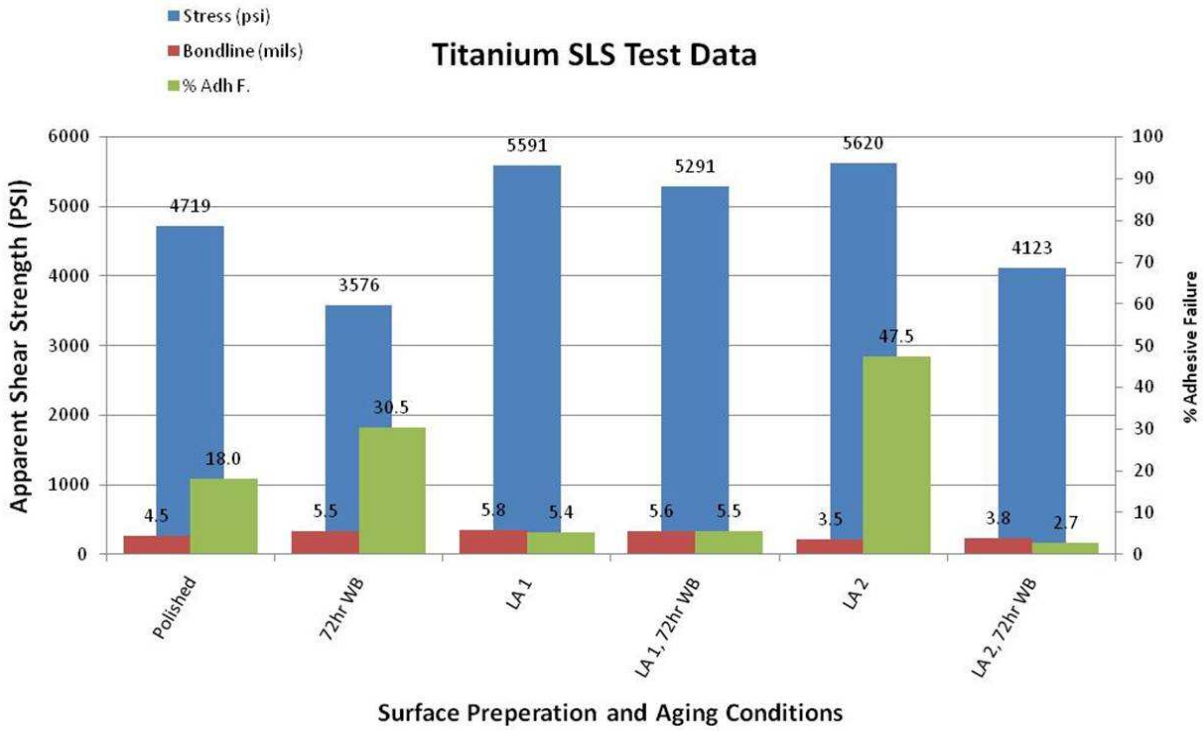

Figure 7: Titanium SLS test results. Immersion in boiling water is denoted by a time in hours and the symbol WB for "water boil." The baseline samples received only surface polishing. The experimental samples are denoted by LA for "laser ablation." LA1 conditions were parallel lines with a 12.7 µm pitch at 1000 mW average power. LA2 conditions were parallel lines with 25.4 µm pitch at 1000 mW average power.

Baseline polished titanium lap-shear specimens showed about 30 to 40% loss in apparent shear strength after immersion in boiling water for one to 10 days. The data for the 6hr WB sample in Figure 7 shows lower than expected apparent shear strength due to the bond line thickness being over the maximum specification of 6 mils (~300 µm). Increased exposure to boiling water caused a clear trend for changing failure mode from cohesive failure (in the adhesive) to adhesive failure. Sample LA1, which received the highest laser power and most dense ablation pattern, displayed an increase in apparent shear strength relative to the baseline and less than a 5% decrease in apparent shear strength after immersion in boiling water for 3 days. The low percent adhesive failure for both samples before and after aging is indicative that the adhesive bond underwent little or no degradation. Sample LA2 also received 1000 mW average laser power, but the pitch of the parallel lines was increased to 25 µm. The increase in percent adhesive failure for the un-aged LA2 specimens may be attributed to a bond line thickness under the specified acceptable range. Visual inspection of the bond failure mode indicated that a large amount of the adhesive had been driven out of the bond line during the curing cycle. This can be seen in specimen 6 of Figure 8 where the E-glass scrim cloth is deformed and pushed out of the bondline.

Table 2: Surface properties of titanium adherends with various surface treatments.

Titanium Surface: pattern pitch, power	**RMS roughness (nm)**	**Water Contact Angle (deg)**	**Surface Energy (dynes/cm)**
As received	620	65	37.5
Polished	50	86	32.0
Polished, Ablated: 12.7 µm, 75 mW	60	44	41.3
LA1: polish, ablate 12.7 µm, 1000 mW	1400	< 5	54.3
LA2: polish, ablate: 25.4 µm, 1000 mW	1000	< 5	54.3
LA3: polish, ablate: 50.8 µm, 1000 mW	650	< 5	54.3

Sample>> Process	1	2	3	4	5	6	7
Ablation(mW)	0	0	75	1000	1000	1000	1000
Pitch (µm)	NA	NA	12.7	12.7	12.7	25.4	25.4
Age (days)	0	3	0	0	3	0	3

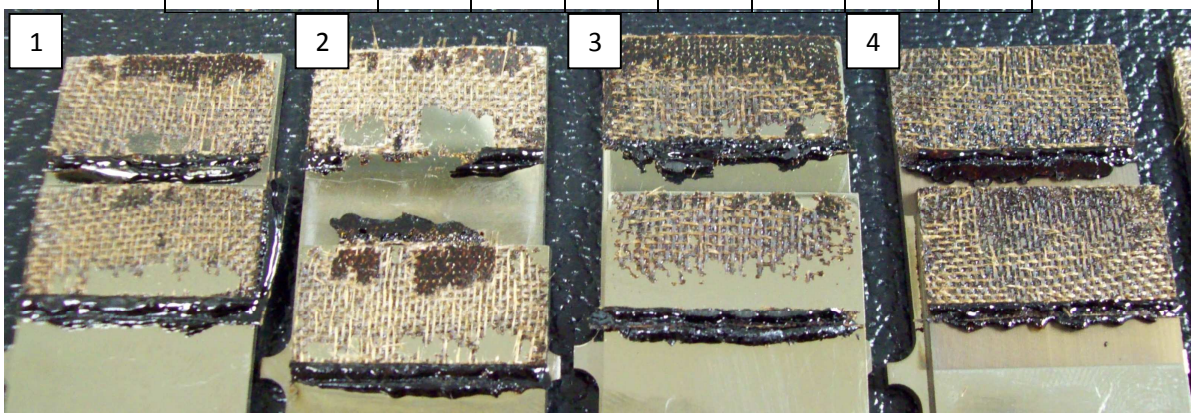

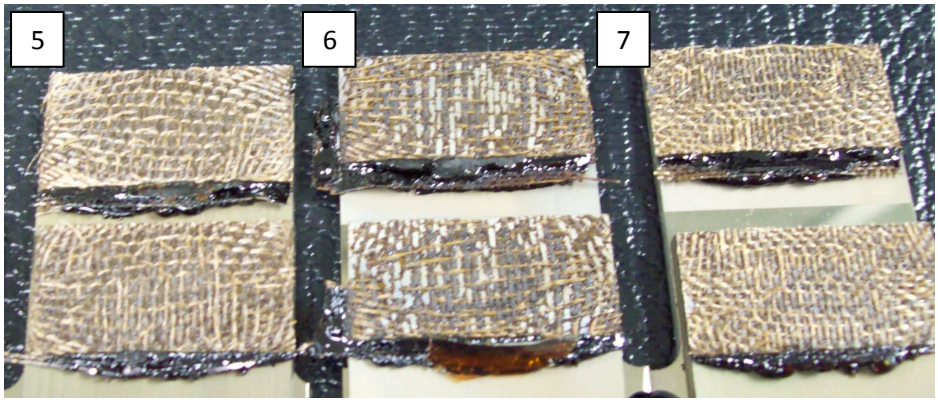

Figure 8: Comparison of titanium lap-shear failure mode. All samples were polished to 50 nm roughness as a first step. The accompanying table describes subsequent processes before the specimens were tested. All ablation patterns were parallel lines running parallel to the specimen tensile test direction.

4.3 Goniometry of Adhesives

Contact angle measurements and surface energy calculations for AF555 and PETI-5 adhesives were performed for comparison with the CFRP and titanium adherends, respectively. The water contact angle and surface energy of AF555 were 80.1° and 31.5 dynes/cm, respectively. Comparison with the data in Table 1 does indicates that uncured AF555 adhesive has similar surface properties to untreated, smooth CFRP adherends. The water contact angle and surface energy for PETI-5 adhesive were 61.7° and 42.5 dynes/cm, respectively. Comparison with the data in Table 2 indicates that PETI-5 has similar surface properties to untreated titanium. PETI-5 should wet titanium spontaneously after ablation at 1000 mW using a pitch of 50.8 µm or denser.

4.4 XPS Analysis

Samples of CFRP material were inspected by XPS after ablation between 0 and 100 mW while holding a constant pitch of 12.7 µm. Samples that received ablation power below or at the ablation threshold showed little or no differentiation. The sample which received 100 mW of average laser power began showing significant changes in the carbon and oxygen composition as shown in Figure 9 and Figure 10. The C1s signal shows a loss of a high binding energy shoulder and a broadening of the main peak for 100 mW relative to all lower ablation powers. The O1s signal shows a significant decrease in signal strength and slight shift to higher binding energy after ablation at a 100 mW. Figure 1111 shows smooth changes in the C1s and O1s signals strengths from a ratio of 3.35 : 1 for unablated CFRP to 5.25 : 1 for CFRP ablated at 100 mW. These changes in surface chemistry indicate that laser ablation causes quantifiable changes in surface chemistry near the ablation threshold when only minor topographical changes are produced. This data suggests that a decomposition of the surface polymers is occurring which causes the loss oxygen containing species such as CO_2 and leaves carbon rich residues on the surface.

XPS of CFRP samples ablated above 100 mW is currently underway to observe the chemical and topographical effects well above the ablation threshold.

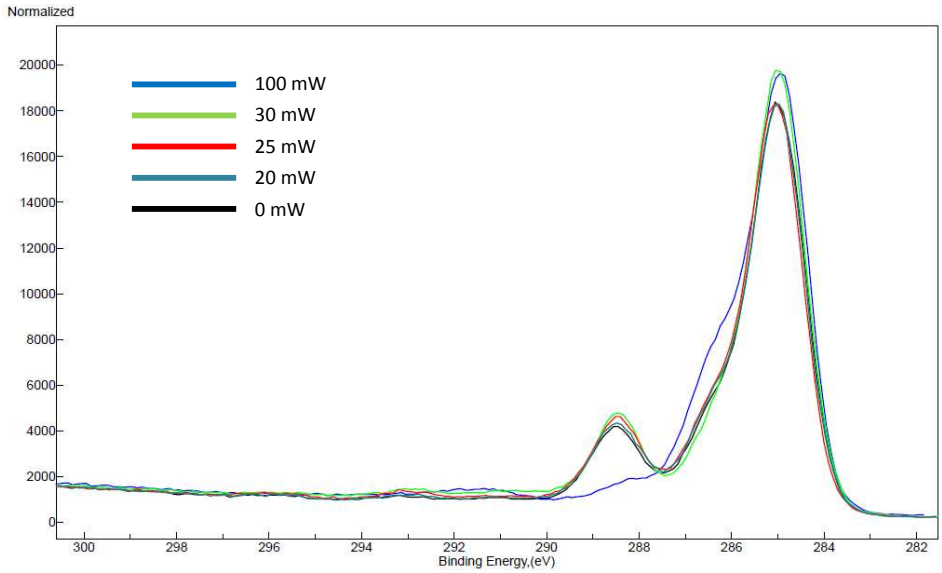

Figure 9 Overlay of high resolution XPS spectra of the C1s state

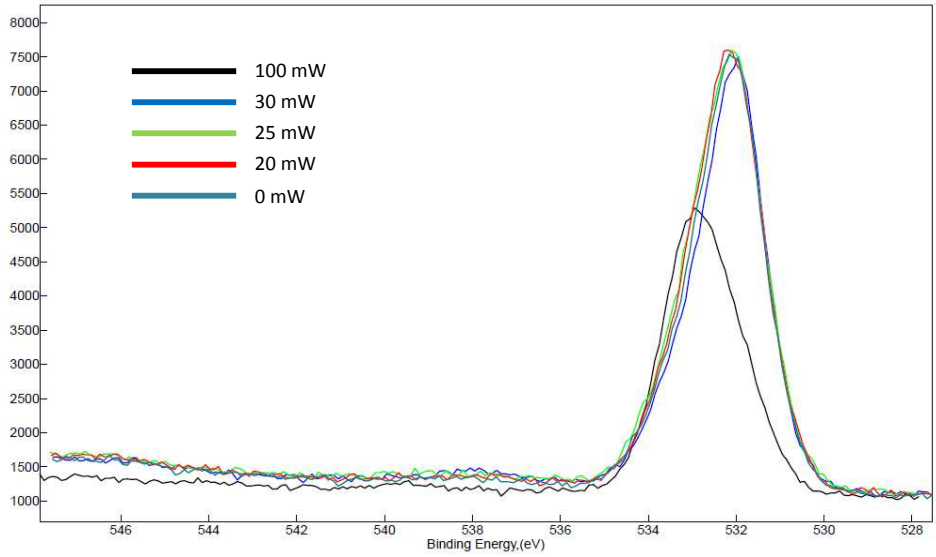

Figure 10 Overlay of high resolution XPS spectra of the O1s state.

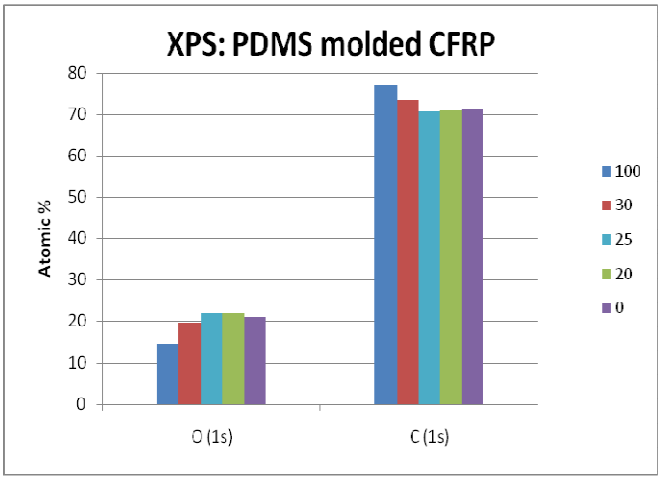

Figure 11: Oxygen and carbon surface content of CFRP sample ablated at various powers**.**

Titanium adherends were inspected by XPS below and above the ablation threshold. Figure 12 shows an overlay of several survey spectra after low power ablation and one spectrum after argon sputtering within the XPS analysis chamber. The overlay spectrum show a small decrease in the titanium oxide and oxygen signals as the titanium (Ti2p3/2, Ti2s) peaks increase. The argon sputtered sample spectrum indicates a dramatic decrease in oxygen content and a concomitant increase in titanium metal alloy (Ti-6Al-4V) at the surface. This indicates that low energy laser ablation under 200 mW has only a minor impact on the oxidative state of a titanium adherend surface.

XPS of Ti samples ablated above 200 mW is currently underway to observe the chemical and topographical effects well above the ablation threshold.

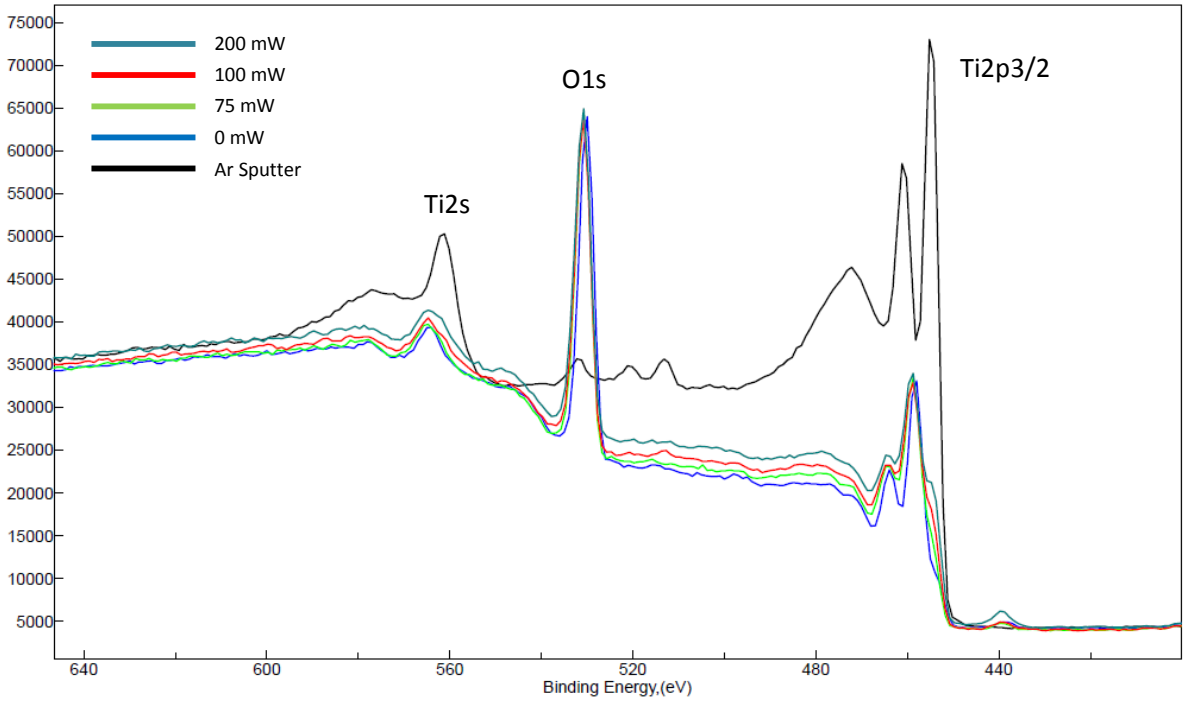

Figure 12: Overlay of Titanium XPS spectra of adherend exposed to laser power near the ablation threshold.

5.0 Conclusions:

The relationship between surface topography and chemical state of a laser modified adherend and bonding performance in single lap joints was investigated. The low energy effects of laser ablation were fully characterized by XPS and goniometry on both titanium and composite adherends. Both materials appear to undergo minimal modification near the ablation threshold. Increased ablation power creates significant changes in topography and increase chemical modification as well as indicated by goniometry results.

Similarities between the surface energy of an adherend and the surface energy of an uncured adhesive did not show any correlation with lap-shear apparent shear strength. The percent adhesive failure correlated well with apparent shear strength and bond line thickness for most titanium specimens bonded with PETI-5 adhesive. Other tests which may be more sensitive to surface modifications are currently being developed. Highly porous bonds made with AF555 adhesive resulted in low strength mechanical test results cannot be correlated directly with other surface/chemical parameters. Other methods of bonding and different adhesive systems are being looked at to improve efficacy of the test.

6.0 Acknowledgements:

This work was carried out in fulfillment of AFOSR contract award number: FA9550-10-1-0386. The authors would like to thank NASA's Langley Research Center and especially the Advanced

Materials and Processing Branch for use of fabrication facilities/materials, time on analytical equipment and access to experienced experts in the field of adhesion science.

7.0 References:

(1) Benard, Q.; Fois, M.; Grisel, M. "Peel ply surface treatments for composite assemblies: chemistry and morphology effects." *Composites: Part A* **2005**, *36*, 1562-1568.

(2) Awaja, F.; Gilber, M.; Kelly, G.; Fox, B.; Pigram, P. "Adhesion of polymers." *Progress in Polymer Science* **2009**, *34*, 948-968.

(3) Liu, H.; Simone, C.; Katiyar, P.; Scola, D. "Adhesive properties of low viscosity phenylethynyl (PE) end-capped *co*-oligomides and *co*-oligomide blends." *Internation Journal of Adhesion and Adhesives* **2005**, *25*, 219-226.

(4) Cherian, J.; Castner, D.; Fisher, R. "Surface analysis of disbonded titanium/sol-gel/polyimide joints." *Journal of Materials Engineering and Performance* **2002**, *11*, 603 - 609.

(5) Belcher, M.; Wohl, C.; Connell, J. "Laser surface preparation and bonding of aerospace structural composites " *17th International Conference on Composite Materials* Edinburgh, United Kingdom, July 27 - 31 (2009).

(6) Belcher, M.; Wohl, C.; Connell, J. "Surface preparation and bonding on composite aircraft." *32nd Annual Meeting of the Adhesion Society* Savannah, GA United States, February 15 - 18 (2009).

(7) Belcher, M.; Wohl, C.; Connell, J. "Surface preparation and bonding on composite aircraft." *NASA Aviation Safety Technical Conference* Denver, CO United States, October 21 - 23 (2008).

(8) Belcher, M.; List, M.; Ghose, S.; Watson, K.; Hopkins, J.; Wohl, C.; Connell, J. "Effect of laser surface preparation and coupling agent composition on durability of adhesively bonded Ti-6Al-4V." *55th International SAMPE Symposium and Exhibition* Seattle, WA United States, May 17 - 20 (2010).

(9) Molitor, P.; Young, T. "Adhesive bonding of titanium alloy to a glass fibre reinforced composite material." *Internation Journal of Adhesion and Adhesives* **2002**, *22*, 101-107.

(10) Lawrence, J.; Li, L. "Wettability characteristics of carbon steel modified with CO2, Nd:YAG, excimer, and high powered diode lasers." *Applied Surface Science* **2000**, *154-155*, 664-669.

(11) Baburaj, E.; Starikov, D.; Evans, J.; Shafeev, G.; Bensaoula, A. "Enhancement of adhesive joint strength by laser surface modification." *Internation Journal of Adhesion and Adhesives* **2007**, *27*, 268-276.

(12) Rotel, M.; Zahavi, J.; Tamir, S.; Buchman, A.; Dodiuk, H. "Pre-bonding technology based on excimer laser surface treatment." *Applied Surface Science* **2000**, *154-155*, 610-616.

(13) Benard, Q.; Fois, M.; Grisel, M.; Laurens, P. "Surface treatment of carbon/epoxy and glass/epoxy composites with an excimer laser." *International Journal of Adhesion and Adhesives* **2006**, *26*, 543 - 549.

(14) Benard, Q.; Fois, M.; Grisel, M.; Laurens, P.; Joubert, F. "Influence of the polymer surface layer on the adhesion of polymer matrix composites." *Journal of Thermoplastic Composite Materials* **2009**, *22*, 51 - 61.

(15) Israelachvili, J. *Intermolecular and Surface Forces*; Academic Press: Amsterdam, 2003.

(16) Busscher, H.; Van Pelt, A.; De Boer, P.; De Jong, H.; Arends, J. "The effect of surface roughening of polymers on measured contact angle of liquids." *Colloids and Surfaces* **1984**, *9*, 319 - 313.

(17) Hergenrother, P. M.; Smith, J. G. Jr. “Chemistry and properties of imide oligomers end-capped with phenylethynylphthalic anhydrides.” *Polymer* **1994**, 35, 4857 - 4864.